Int J Thermophys (2009) 30:77–97
DOI 10.1007/s10765-008-0490-1

Low-Temperature Blackbodies for IR Calibrations in a Medium-Background Environment

S. A. Ogarev · M. L. Samoylov · N. A. Parfentyev · V. I. Sapritsky

Published online: 23 October 2008
© Springer Science+Business Media, LLC 2008

Abstract Utilization of Earth remote-sensing data to solve scientific and engineering problems within such fields as meteorology and climatology requires precise radiometric calibration of space-borne instruments. High-accuracy calibration equipment in the thermal-IR wavelength range ought to be combined during calibration procedures with the simulation of environmental conditions for space orbit (high vacuum, medium background). For more than 35 years, VNIIOFI has developed and manufactured standard radiation sources in the form of precision blackbodies (BB) functioning within wide ranges of wavelengths and working temperatures. These BBs are the spectral radiance and irradiance calibration devices in the world's leading space research institutions, such as SDL (USA), DLR (Germany), Keldysh Space Center (Russia), RNIIKP/RISDE (Russia), NEC Toshiba Space Systems (Japan), etc. The paper contains a detailed description of low-temperature precision BBs developed at VNIIOFI. The characteristics of variable-temperature (100 K to 400 K) research-grade extended-area (up to 350 mm) BB models BB100-V1 and BB-80/350 are described (they are intended for radiometric calibrations by comparison with a primary standard source), as well as those that can be used as sources for high-accuracy IR calibration of space-borne and other systems not requiring a vacuum environment. The temperature nonuniformity and stability of these BBs are (0.05 to 0.1) K (cavity-type BB100-V1), and 0.1 % for the (1.5 to 15) μm wavelength region under cryo-vacuum conditions of a medium-background environment.

Keywords Blackbody · Emissivity · IR calibration · Long-term stability · Low temperature · Medium-background environment · Reproducibility of measurements

S. A. Ogarev (✉) · M. L. Samoylov · N. A. Parfentyev · V. I. Sapritsky
All-Russian Research Institute for Optical and Physical Measurements (VNIIOFI),
46 Ozernaya, 119361 Moscow, Russia
e-mail: ogarev-m4@vniiofi.ru

1 Introduction

The solution of many important problems of space technology, space and astrophysical research, ecology, reliable weather prediction, and the monitoring of climatic changes on the Earth are directly connected with ensuring the uniformity of measurements in the framework of the Global Earth Observation System (GEOSS) by means of a unified radiometric scale [1]. The accuracy of measurements (e.g., the temperature of the ocean surface) required for monitoring and predicting climatic changes is 0.1 K. Hence, there are high demands on the accuracy of the preflight and in-flight radiometric calibration of the space-borne instruments, particularly within the IR range of wavelengths [2].

To meet the requirements, strict specifications are placed on the reproducibility and accuracy of the equipment used for radiometric measurements. According to USA specialists, the reproducibility of absolute measurements within the wavelength range from 0.2 μm to 15 μm must not exceed 0.01 K over a 10-year time period.

Most Russian state radiometric, photometric, and spectral standards, as well as the thermodynamic temperature scale, are based on standard optical sources of the "blackbody" (BB) type [3] that have been developed by VNIIOFI since the 1970s. This approach reflects the preference for the "radiation" approach by the Russian metrological school in the field of optical radiometry, mostly due to the reason that there is a substantial reduction in the uncertainty of spectral components of incoherent optical radiation from "calculated" radiation sources compared to reference lamps. In addition to Russian standards, the national standards of the key world metrological centers, such as NIST (USA), PTB (Germany), NPL (UK), etc., make use of BBs developed and fabricated by VNIIOFI [4]. The practical implementation is based on a series of VNIIOFI-developed cavity and plane-type BBs, both of the variable-temperature type and those based upon fixed points corresponding to phase transitions of pure metals and metal–carbon and metal–metal alloys.

The radiation from a perfect cavity-type source regarded as an absolute BB does not depend on the cavity shape or the properties of its wall materials and, according to Planck's law, is completely determined by its temperature. As a thermal radiation source, a cavity-type BB has a number of advantages over other thermal sources—these include higher reproducibility and lower dependence of the effective emissivity ε_λ on variations and degradation of the optical properties of the cavity's inner surface.

The development of state-of-the-art technologies and optics calls for increasingly accurate blackbody radiometry as well as the practical implementation of the spectral radiance and spectral irradiance scales, which currently have a reproducibility of about 0.1 %. One of the fundamental tasks of radiometry is the development of a new generation of BB sources for the implementation of scales with total uncertainties <0.1 % [3].

Since its founding in 1971, VNIIOFI's Optical Radiometry and Photometry Division (formerly a laboratory) has been developing BB sources for the entire IR-visible spectral range [5–8]. The basic characteristics of most low-temperature BB radiation sources developed at VNIIOFI are given in Table 1 as functions of the required spectral range and radiation flux density in accordance with the working temperatures from cryogenic (down to 200 K) to the (200 to 450) K temperature range. We describe

in this paper both basic types of low-temperature BBs implemented at VNIIOFI: variable-temperature and fixed-point phase transitions of pure materials (Ga and In and binary metal–metal eutectic alloys). The low-temperature BBs were developed for the calibration of IR instruments under cryo-vacuum conditions emulating the orbital working environment. Copper and aluminum alloys are used as the radiation cavity materials for the low-temperature and cryogenic BBs. The required value of emissivity, ε_λ, is achieved by using different black coatings, in particular, Chemglaze Z-302 for BB29gl [6] and Nextel Velvet 811-21 for BB100, BB100-V1, and BB-80/350.

2 BB Radiation Sources in the (100 to 1,000) K Range for Precision Calibration of Space-Borne Instruments

2.1 BB General Background and Design Concepts

The use of precise, highly-stable standard BB sources in the IR and visible ranges of wavelengths is important for the preflight calibration of space-borne radiometric equipment [5,6]. The admissible uncertainty and long-term stability of measurements should not exceed 0.1 % and 0.02 % per decade in the (0.2–3) µm spectral range, and 0.1 K and 0.01 K per decade in the (3 to 15) µm range [7].

Within the last 10 years, VNIIOFI has developed a number of unique precision BBs (including those operating at low temperatures), which are described in detail in [5,8], to meet these requirements. As shown in Table 1, VNIIOFI developed fixed-point sources based on gallium and indium phase transitions, as well as vacuum variable-temperature BBs for the ranges (80 to 300) K, (100 to 400) K, (240 to 350) K, and (400 to 1,000) K, for precision calibration in the IR-range of (1.5 to 15) µm for various research institutions—the German Aerospace Centre (DLR) and PTB in Germany, NPL in the UK, Space Dynamics Lab (SDL) in the USA, NEC TOSHIBA Space Systems and JAXA in Japan, NIM and IAO in China, and RNIIKP in Russia—as well as in cooperation with the Keldysh Space Centre in Russia.

VNIIOFI developed, for cryo-vacuum operating conditions of IR-sensors, wide-aperture (apertures from 100 mm to 350 mm) BB models BB100, BB900, BB1000, BB100-V1, and BB-80/350, which can also be used for operation in normal atmospheric conditions. The uncertainty of thermodynamic temperature reproduction by BB100, BB900, BB1000, and BB100-V1 sources within the entire working temperature range does not exceed 0.5 K (1σ).

BB radiation source BB1000 [5,6] has a graphite bottom with V-shaped grooves and is cooled with a gold-plated composite reflector. Cavities BB100, BB900, and BB1000 are resistively heated. The design of BB100, BB900, BB1000, and BB100-V1 utilized computer simulation of the optical properties of the internal surfaces of the radiation cavities by the Monte-Carlo method [9] with the use of STEEP software [10], with an absolute error of the calculations of 10^{-5}, which makes it possible to optimally select the bottom coatings of cavities with V-shaped grooves or reflecting lateral walls. The second stage dealt with BB cavity heat transfer by radiation and thermal conductivity. Mathematical modeling was based on the Poisson differential equation with corresponding boundary conditions. Boundary conditions of first order (temperature provided) have been used to describe the contact of the blackbody components

Table 1 Characteristics of main low-temperature BB radiation sources developed in VNIIOFI

Type	Temperature (K)	Radiating cavity	Cavity dimensions (mm)	Opening (mm)	Emissivity	Consumed power (kW) max	Year of development
BB1000 (vacuum)	400–1000	Graphite V-grooved bottom, gold-covered aluminum lateral walls	80 × 80	32	>0.99(2.7 μm–5.5 μm)	0.3	2000
BB156in	429.75	Copper cavity in Indium fixed-point cell	172 × 34	20	0.9998(1 μm–20 μm)		2000
VTBB	330–380/210–350/ 320–450	Copper	250 × 40	8/30/20	0.9998(1 μm–20 μm)		1998/2002
BB29gl	302.9	Copper cavity in Gallium fixed-point cell	172 × 34	8 / 20	0.9998(1 μm–20 μm)	0.1	1995
BB300	80–300	Copper	500 × 140	60	0.9997(1 μm–20 μm)	0.1	1992
BB900 (vacuum)	400–900	Aluminum alloy	190 × 160	100	0.992	1	1997
BB100-V1 (vacuum)	240–350	Copper with Nextel Velvet 811-21 coating; V-grooved bottom	200 × 120	100	0.997(1.5 μm–15 μm)	3	2005
BB80–350	220–350	Copper with Nextel Velvet 811-21 coating;	Ø 350	Ø 350	0.96 ± 0.02	0.8	2006
BB100 (vacuum)	100–400	Aluminum alloy	190 × 160	100	0.999	1	1997

with the tank of liquid nitrogen. The Stefan–Boltzmann law has been used to define boundary conditions of the second order. Computer thermophysical simulation using the ANSYS 8.0 program [11] was carried out for BB100-V1.

2.1.1 Choice of Cavity Shape and Effective Emissivity Modeling

To meet the most common customers' requirements for accuracy and long-term stability of measurements, designs of the cavity type can be seen in high-precision unique BBs developed within the last decade at VNIIOFI [3,8]. Among them there are variable-temperature and fixed-point models BB100, BB300, BB900, BB1000, VTBB, BB29Ga, BB156In, and BB100-V1 within the 100–1000 K working temperature range, and they are designed for the calibration of space-borne IR sensors and high-precision radiometry at such research organizations as the German Aerospace Center (DLR) and Physikalisch-Technische Bundesanstalt (Germany), National Physical Laboratory (UK), Space Dynamics Lab (USA), and NIM and IAO (China).

As an example, for BB100-V1, we selected a cylindrical cavity because, for this shape, the selected method of thermostabilization is simply implemented by enveloping the tube with liquid. Due to the relatively small required field of view (FOV) of 0.012 mrad, the radius R of a cavity should not be significant greater than the aperture radius, $R_a = 50$ mm. We have chosen $R = 60$ mm and cavity depth $L = 200$ mm. It is known that the normal effective emissivity of a cylindrical cavity with a flat bottom sharply decreases if the surface of the bottom has a specular component of reflection. To avoid this effect, we use concentric grooves on the cavity bottom. We considered the grooves of a trapezoidal profile, with the height and step of the grooves equal to 5 mm, and with flat tops and bottoms of 0.2 mm width. For the given FOV, only the bottom (excluding its narrow peripheral annulus) is viewable.

An important special case of the local directional effective emissivity is the local normal effective emissivity $\varepsilon_{e,n}(r, \lambda, T_{ref})$. It corresponds to viewing the aperture of an axi-symmetric cavity along an infinitely thin ray passing parallel to the cavity axis and crossing the aperture plane at the point with radial coordinate r. The average normal effective emissivity $\varepsilon_{e,n}$, which is used in typical calibration arrangements, can be considered as an average over the cavity aperture. By analogy, the average directional and conical effective emissivities can be introduced.

The computation of the effective emissivity for blackbodies under development was performed by means of the STEEP3 modeling software [10], based on the Monte-Carlo algorithm [9,12,13] that is briefly depicted below. The analysis is restricted to the case of the uniform specular-diffuse reflection model that assumes:

(i) The surface emits diffusely (according to Lambert's law), with an emissivity ε.
(ii) The hemispherical reflectance $\rho = 1 - \varepsilon$ does not depend on the incidence angle and is the sum of two components—specular ρ_s and diffuse ρ_d.
(iii) The surface diffusity defined as $D = \rho_d/\rho$ does not depend on the incidence angle.

Moreover, the validity of the ray optics approximation is assumed, diffraction effects are considered negligible, and radiation is entirely depolarized due to multiple reflections.

The Monte-Carlo method of radiation transfer simulation is based on a ray-tracing algorithm. For the calculation of the effective emissivity of the cavity by the Monte-Carlo method, the radiative flux is represented by a large number of rays moving along rectilinear trajectories. The radiation heat transfer inside the cavity is simulated by a random Markov's chain of reflections of these rays from the internal cavity surface. To reduce the dispersion of the calculation and decrease the computing time, the method of statistical weights was used.

For the calculation of the effective emissivity, the optical reciprocity theorem and the technique of inverse ray tracing were used. The rays with a statistical weight of unity were directed from a point of observation toward the opening of the cavity, and their history was followed until they escape from the cavity or until their statistical weight became less than the given truncation value, δ. The last point of reflection is considered as the point of birth of the ray propagating in the inverse direction.

The spectral radiance along the ray exiting from the cavity opening is proportional to

$$\varepsilon_1 P(\lambda, T) + \rho_1(\varepsilon_2 P(\lambda, T_k) + \rho_2(\varepsilon_3 P(\lambda, T_k) + \rho_3(\varepsilon_4 P(\lambda, T_k) + \ldots)\ldots)) \quad (1)$$

where ε_k, ρ_k, and T_k are the spectral emissivity, spectral reflectance, and temperature of the cavity wall at the point of the kth reflection, respectively; $P(\lambda, T)$ is Planck's function.

After choosing the reference temperature T_{ref}, it is possible to evaluate the effective emissivity of the cavity by following the histories of a large number of rays, n, the direction of which are chosen randomly following the given conditions of observation:

$$\varepsilon_{\mathrm{e}}(\lambda, T_{\mathrm{ref}}) = \frac{1}{nP(\lambda, T_{\mathrm{ref}})} \sum_{i=1}^{n} \sum_{j=1}^{m_i} \varepsilon_j P(\lambda, T_j) \prod_{k=1}^{j-1} \rho_k, \quad (2)$$

where m_i is the number of reflections of the ith ray trajectory. With $\delta = 10^{-5}$ and $N = 10^6$, the uncertainty of the effective emissivity calculation is $\Delta\varepsilon_{\mathrm{e}} \approx 0.0001$.

We have computed (using STEEP3 [10]) the normal effective emissivities of an isothermal cylindrical cavity with a flat bottom featuring concentric V-grooves. We have used the limiting values of the wall emissivity (0.935 and 0.990) and four values of the wall diffusity. The results of the computations are presented in Table 2.

As an example, for blackbody BB100-V1 (see Sect. 2.2), we have computed the normal spectral effective emissivities for two limiting values of the cavity wall emissivity

Table 2 Normal effective emissivity of a BB100-V1 isothermal cavity

Cavity wall emissivity	Cavity wall diffusity			
	0.7	0.8	0.9	1.0
0.935	0.9972	0.9976	0.9980	0.9983
0.990	0.9996	0.9996	0.9997	0.9997

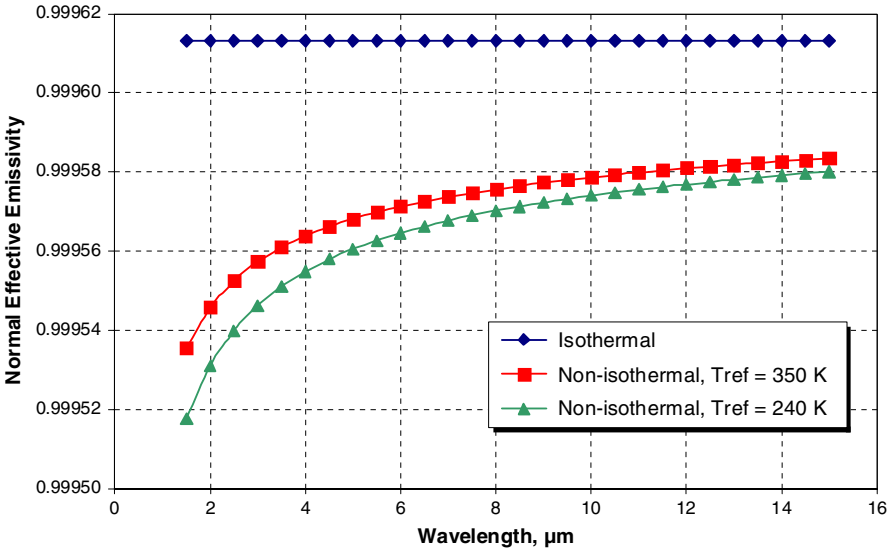

Fig. 1 Normal spectral effective emissivity of BB100-V1 for three temperature distributions; wall emissivity is 0.990

(0.935 and 0.990) and two temperature distributions obtained by the FEA for two temperatures of the thermostatting liquid (350 K and 240 K). The environmental temperature in all cases is 77 K; the diffusity of the cavity walls is 0.7. The results of the computations are depicted in Fig. 1. The data analysis and numerical experiment additionally performed show that these values of the effective emissivity do not change significantly for oblique viewing up to angles of $\pm 4.5^\circ$ with respect to the cavity axis. No background radiation effects were detected.

2.1.2 Steady-State Temperature Distribution Finite-Element Analysis (FEA)

It is necessary to evaluate the temperature distribution over the internal surface of a cavity. The temperature significantly depends upon design features that determine all heat sources and sinks. We have built the simplified thermophysical model of a BB100-V1, as an example. We have assumed that the temperatures of the edge of the stainless-steel holder and the brass thermal link are constant and equal to the environmental temperature T_e. The heat released in ring zones propagates through the copper cavity, brass thermal link, and stainless-steel holder. The internal surface of a cavity loses heat due to radiative heat transfer through the cavity aperture. We have assumed that there are no conductive heat losses through the thermal insulation.

Let us assume that there is no heat exchange among points placed on a cavity internal surface due to its very small temperature nonuniformity. The heat-flux density that leaves a point on a cavity internal surface at temperature T and escapes through the edge cut of a stainless-steel hood directly or after one or more reflections is equal to

$$q = \varepsilon\sigma \left(T^4 - T_e^4\right) F, \tag{3}$$

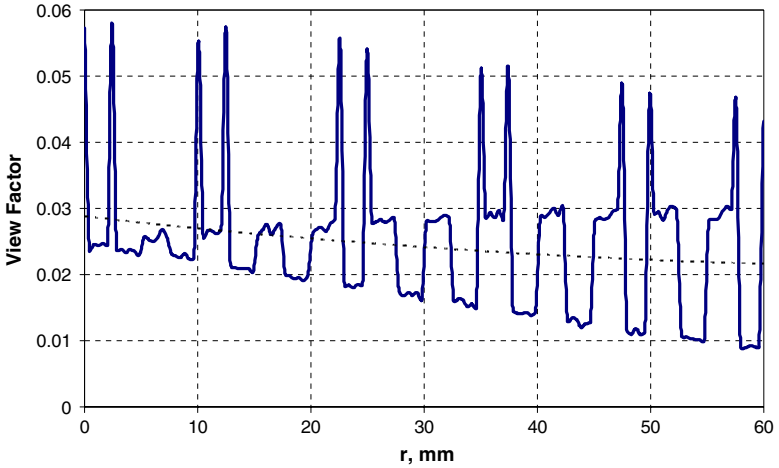

Fig. 2 Distribution of resolving view factors along the radius of cavity bottom

where ε is the total hemispherical emissivity, $\sigma = 5.6704 \times 10^{-8}\ \mathrm{W \cdot m^{-2} \cdot K^{-4}}$ is the Stefan–Boltzmann constant, T_e is the environmental temperature, and F is the resolving view factor between that point and the hood's edge cut.

The view factor between surfaces A_1 and A_2 is defined as the ratio of radiant power emitted by A_1 to the radiant power falling onto A_2 directly and after every possible reflection from A_1 and all intermediate surfaces [14]. To compute the resolving view factors from a point on the internal cavity wall to the edge cut of the stainless-steel hood, we used the customized version 4V of the STEEP3 program. The algorithm employed is based on the calculation of statistical weights of rays emitted by the given point on the cavity generatrix and escaping through the hood's opening.

The computed distribution of resolving view factors along the radius of a cavity bottom is presented in Fig. 2. The peaks belong to flat areas in the peaks and valleys of the concentric grooves, the lower plateaux—to internal and external sloping surfaces. The dashed line depicts the trend obtained by the moving average method. The distributions presented in Fig. 2 were used for finite-element modeling of the steady-state temperature distribution along the cavity internal surface.

We used the FEA program ANSYS 8.0 [11] and the thermophysical model depicted above, together with the following parameters:

- Thickness of bottom—15 mm
- Thickness of cylindrical walls and diaphragm—12 mm
- Stainless-steel holder thickness—1 mm
- Brass heat-link thickness—1 mm
- Total thickness of black coating and primer—0.1 mm

We used the following values of thermal conductivity, k, for the materials employed:

- Copper, $k_{Cu} = 393\ \mathrm{W \cdot m^{-1} \cdot K^{-1}}$
- Brass, $k_{Br} = 130\ \mathrm{W \cdot m^{-1} \cdot K^{-1}}$

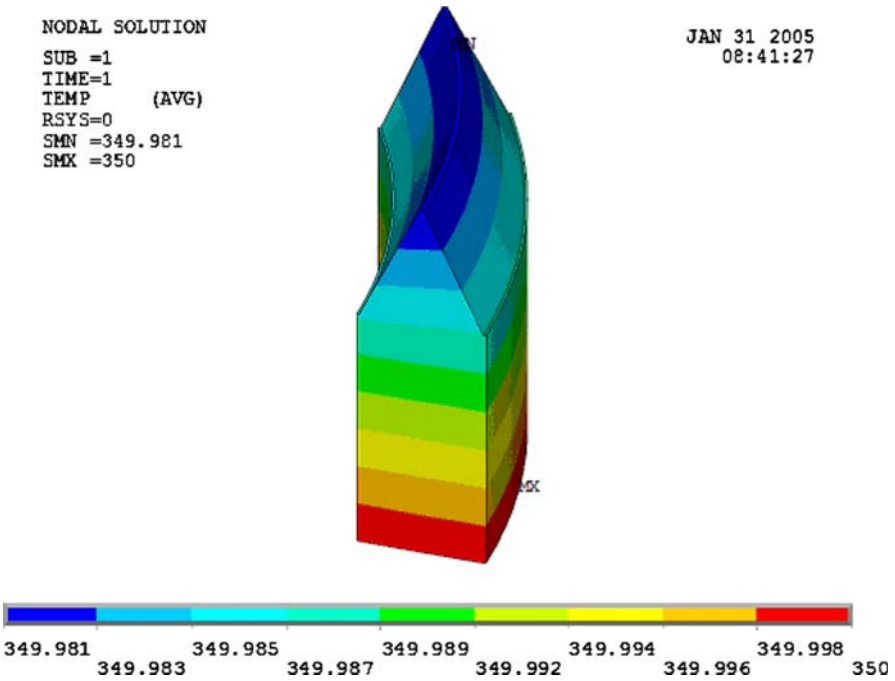

Fig. 3 Steady-state temperature distribution across the "tooth" on the cavity bottom

- Stainless steel, $k_{SS} = 15\,\mathrm{W}\cdot\mathrm{m}^{-1}\cdot\mathrm{K}^{-1}$
- Black coating and ground, $k_b = 1\,\mathrm{W}\cdot\mathrm{m}^{-1}\cdot\mathrm{K}^{-1}$

At the first stage, we supposed that the bottom has no grooves. For modeling, we employed multilayer shell finite elements of triangular shape. Finally, we built the solid finite-element model of a "tooth"—a selected annular area of a grooved bottom. Because the estimated radial temperature gradient along the bottom is negligible (about 4 mK), we considered the vertical cylindrical surfaces to be adiabatic. On the flat and inclined surfaces of a "tooth," the radiative heat losses were determined according to Fig. 2 and Eq. 3. The computed temperature drop (see Fig. 3) does not exceed 4 mK. The average temperature of the grooved surface differs from the temperature of the surrounding liquid by approximately 15 mK.

2.1.3 Black Coating Selection

While identifying an appropriate coating for the bottom of a low-temperature blackbody intended for operation in a vacuum environment, we were looking for black materials or paints possessing an emissivity better than 0.9 in the spectral range of interest, as well as low out-gassing properties. There are several comprehensive reviews [15–17] on the application and optical properties of black paints and various coatings suitable for stray light suppression, solar energy absorption, for thermal detectors of

optical radiation, radiation loss control, etc. After a comparative analysis of literature data, Nextel (formerly 3M) Velvet Coating 811-21 was chosen.

This black coating has been used extensively in infrared radiometry for more than 25 years [18–21] and it can be exploited for the cryo-vacuum environment. Moreover, VNIIOFI has broad experience with its use in a variety of radiometric systems. The spectral emissivity of Nextel 811-21 is depicted in [20,21]. The curve obtained by PTB (Germany) [21] is the spectral normal emissivity; another curve obtained by BNM/LNE (France) [20] is the spectral directional emissivity for an angle of 12° with respect to the normal. Only the BNM/LNE curve [20] spans the entire spectral range of interest. The spectral dependences are obtained under different measurement conditions, and the coatings are laid on various substrates. Furthermore, the optical properties of the paint depend substantially upon the style of its application. For our purposes, it is enough to assume that the spectral hemispherical emissivity of Nextel 811-21 is within 0.935 to 0.990 for the wavelength range from 1.5 µm to 15 µm.

The measurements of reflectance performed for the predecessor of Nextel 811-21, the 3M Velvet Black [16], show the presence of a small specular component, <10 % of the overall hemispherical reflectance; the diffuse component of reflectance has a near-Lambertian BRDF [17]. Nextel® Velvet Coating 811-21 can be purchased from Mankiewicz Gebr. & Co [22].

2.2 BB100-V1

The precision large-area low-temperature blackbody model BB100-V1, intended for use as a reference temperature radiation source for the calibration of space-borne radiometers and thermometers in the IR wavelength range from 1.5 µm to 15 µm, was developed for NEC TOSHIBA Space Systems and JAXA (Japan) and the Keldysh Space Center (Russia) in 2005 [2,23]. The BB100-V1 blackbody has a copper cylindrical cavity, painted inside with "NEXTEL Velvet 821-11" black coating, to guarantee the bottom possesses an emissivity better than 0.9 in the spectral range of interest. The blackbody consists of three main parts: the central cylindrical part (radiating cavity), and the rear and front flanges. The outer diameter of the blackbody housing is 214 mm, and the length of the radiating cavity is 200 mm. The overall length of the BB100-V1, including the nozzles (nuts) of copper heat exchanger tubing, is 500 mm. A cross section of the blackbody is shown in Fig. 4. Temperature control of the BB100-V1 uses a liquid circulation-type thermostat PR-1845 from LAUDA (Dr. R.Wobser Gmbh & Co., Germany) with the heat-transfer liquid KRYO-51 (Polydimethylphenylsiloxane) with a (−45 to 200) °C working temperature range. The customer's requirementsd of 20 m overall length of tubing (metal sylphon tubing for placement inside the vacuum chamber and vyton polymer pipes outside the chamber) were also satisfied. The radiating cavity of the BB100-V1 blackbody features a cylindrical shape of 120 mm diameter and 2260 cm^3 volume. The screen-vacuum insulation around the black radiating cavity is made of multilayered polyethylene terephthalate film. The BB100-V1 is assembled in an external housing made of stainless steel. The view of the radiating cavity with external housing and screen-vacuum insulation is presented in Fig. 4.

The radiating cavity of the BB100V1 blackbody contains five PRT-100 type MINCO resistors (Mod. S1059PA5X6, 1 pc., and Mod.S278PD06, 3 pc.) as the temperature

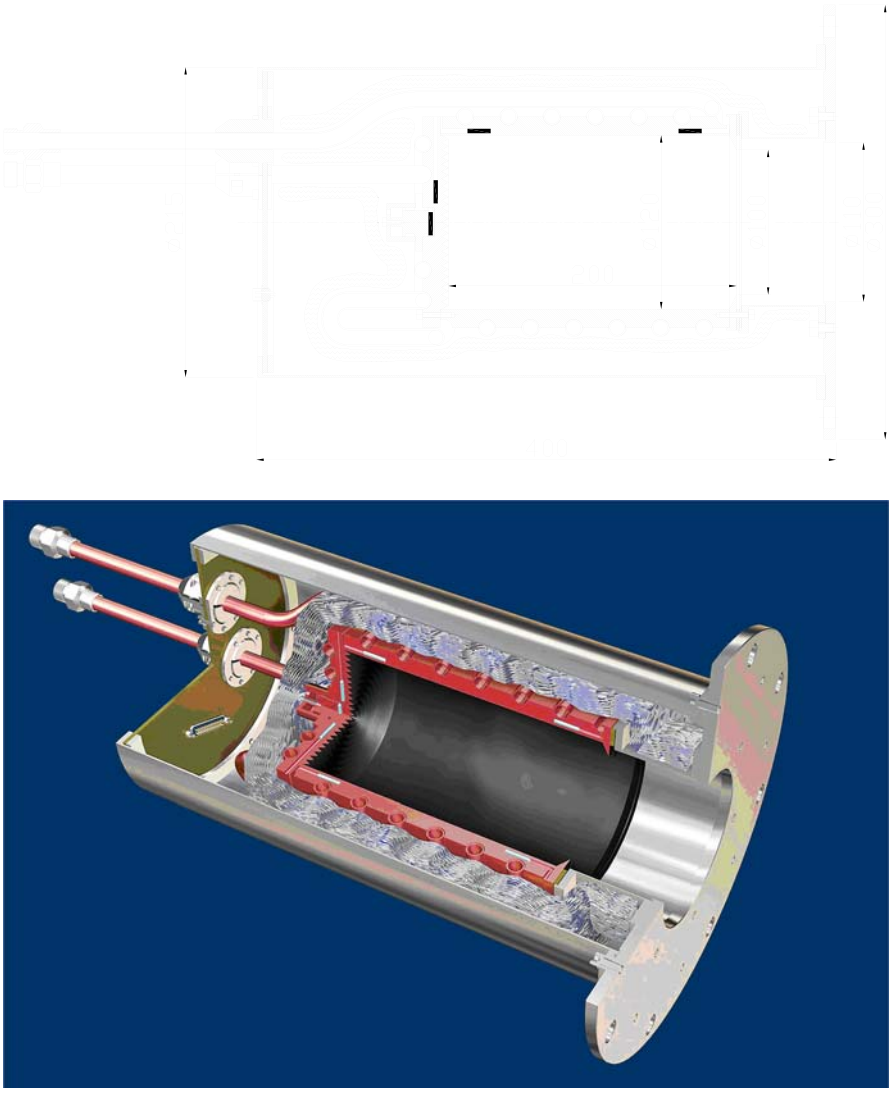

Fig. 4 Cross section and 3D view (computer AutoCAD simulation) of BB100-V1 blackbody

sensors. Three of them are incorporated in the back side of the V-grooved copper bottom, and two others in the cylindrical walls. Four of the sensors are connected to an external multimeter (HP-34970A) via a 25 pin electrical connector placed at the rear flange of BB100V1, with a four-wire scheme for measurement of the electrical resistance. The 5-th sensor is in the feedback loop of the temperature stabilization system based on the LAUDA controller head. The reference PRT-100 temperature sensor was made removable with a special holder to have the possibility of recalibration from time-to-time; it is placed in the center of the external (back) side of the V-grooved bottom of the radiating cavity of the BB100-V1. Specially-designed

software "BB100-V1.EXE" intended to monitor the temperature of the radiating cavity of blackbody BB100-V1 was developed based on LabView software.

2.2.1 Results of BB100-V1 Tests in Cryo-Vacuum Conditions of Space Chambers in Keldysh Center (Russia) and NEC-Toshiba Space (Japan)

From June to August of 2005, the BB100-V1 blackbody was tested under vacuum conditions in a space chamber for temperature stabilization at several set-point values within the −30 °C to +80 °C temperature range. Testing conditions were as follows:

Air pressure (vacuum) inside chamber:	up to 2×10^{-6} torr
Temperature of environment:	from 20 °C ("warm" chamber) to −196 °C
Points of BB100-V1 testing:	−33 °C, 0 °C, +30 °C, +77 °C.

The basic features of the BB 100-V1 based on the tests in cryo-vacuum chambers (both in Russia and Japan) are presented in Table 3. Blackbody BB100-V1 was installed horizontally inside the cryo-vacuum chambers at NEC Toshiba Space Systems and Keldysh Space Center with the possibility of mounting via the front flange to the customer-owned equipment. A schematic of the connections for the temperature control system of the BB100-V1 blackbody is depicted in Fig. 5.

During tests at the Keldysh Space Center, BB100-V1 was placed inside the vacuum chamber in a position contrary to the viewing IR window of the chamber. This was done to have the possibility of scanning the temperature distribution across the BB opening by means of a thermal imager (AGA-780) placed in the vicinity of the IR-window outside the chamber. A visual representation of sample scans across the BB100-V1 aperture obtained in the cryo-vacuum chamber cooled with LN_2, is shown in Fig. 6.

Operation of the temperature-monitoring system of BB100-V1 was tested at set-point temperatures of −33 °C (240 K), 0 °C, +30 °C, and +77 °C (350 K). During the tests, the temperature of the blackbody cavity was measured in the four PRT-100 locations as a function of time. The results are presented in Fig. 7. The blue curve in the plots corresponds to the signal of the PRT sensor located in the lateral wall of the BB100-V1 cavity in the vicinity of its output aperture. Based on an analysis of the measurement data from the PRT-100 temperature sensors incorporated in the cavity of the BB100-V1 blackbody, the following summary was obtained:

(1) Temperature nonuniformity of the BB100-V1 cavity does not exceed:	
Across the cavity bottom:	0.04 °C (K),
Along the cavity wall:	0.1 °C (K).
(2) Warm-up time to set-point value:	
"Warm" vacuum environment ($P = 2 \times 10^{-2}$ Torr; $T_{environment}$ = 20 °C)	
at $T_{initial}$ = 20 °C, T_{end} = 30 °C	time = 40 min;
"Cold" vacuum environment (P = 10^{-6} Torr; $T_{environment}$ = −196 °C)	
at $T_{initial}$ = 30 °C, T_{stab} = −33 °C	time = 80 min;
at $T_{initial}$ = −33 °C, T_{stab} = 0 °C	40 min;
at $T_{initial}$ = 0 °C, T_{stab} = 30 °C	31 min;
at $T_{initial}$ = 30 °C, T_{stab} = 77 °C	44 min.

From the analysis of the measurement data from the PRT-100 temperature sensors incorporated in the cavity of the blackbody, the uncertainty of the thermodynamic temperature reproducibility of the BB100-V1 within the working temperature ranges

Table 3 Technical features of BB100-V1 blackbody

Parameter	Tested value
Operating temperature range	350 K (77 °C)–240 K (−33 °C)
Spectral range	1.5 µm – 15 µm
Cavity effective emissivity	0.997 ± 0.001 (Estimated from computer modeling by STEEP3 software)
Opening (nonprecision aperture)	Ø100 mm
System field-of-view (FOV)	12 mrad (0.688 °)
Environment operation conditions	Vacuum chamber (10^{-6} Torr, below 100 K) Tests were carried out in two modes: (1) "warm" vacuumized chamber ($P = 10^{-2}$ Torr); and (2) "cold" vacuumized chamber ($P = 10^{-6}$, $T = -196$ °C) Air environment (clean room at 23 ± 3 °C)
Temperature nonuniformity across opening	0.04 K, Measured by internal temp. sensors of cavity bottom
Temperature set point resolution	0.01 K
Maximum temperature instability under thermostabilization	±0.02 K, Measured by internal temp. sensors of cavity bottom during 1-h measurement
Limitation on the blackbody warning-up time (approx.)	40–80 min
Total wattage (approx.)	1600 W (switchable to 3500 W with usage of thermostat LAUDA Proline PR1845 LCK 1891)
Input voltage	200 V AC with additional 200–220 V transformer
Blackbody temperature set up and control	External controller of thermostat LAUDA Proline PR1845 LCK 1891 and one PRT-100 sensor incorporated in cavity bottom of BB100-V1; RS-232 interface to PC computer
Type of temperature sensor for control	PtRTD by MINCO Products, Inc., USA: Precision temperature 100-Ohm sensors Mod.S278PD06 (4 pcs.) and Mod. S1059PA5X6 (1 pc.)
Calibration traceability of Pt RTD to NIST	Calibration traceability to NIST is assumed for 1 (one) Pt RTD only
Operating environment pressure	10^{-6} Torr
Cable length	5 m for inside vacuum chamber and 5 m for outside chamber

did not exceed 0.5 K (1σ). The temperature nonuniformity and long-term stability are <0.1 K and 0.1 % for the 1.5 µm to 15 µm wavelength region under the cryo-vacuum conditions of a medium-background environment.

2.3 Plane-Type Radiation Source BB-80/350

A standard thermal radiation source of extended type, BB-80/350 (hereafter referred to as BB-80/350), was designed for the ground-based preflight radiometric calibration of space-applied equipment in the (2.5 to 15) µm range. BB-80/350 comprises, in essence, a thermal radiation source, a thermal controlling system, and a system for monitoring the radiation source parameters. The BB-80/350 diagram and layout are given in Fig. 8. BB-80/350 basic characteristics are given in Table 4.

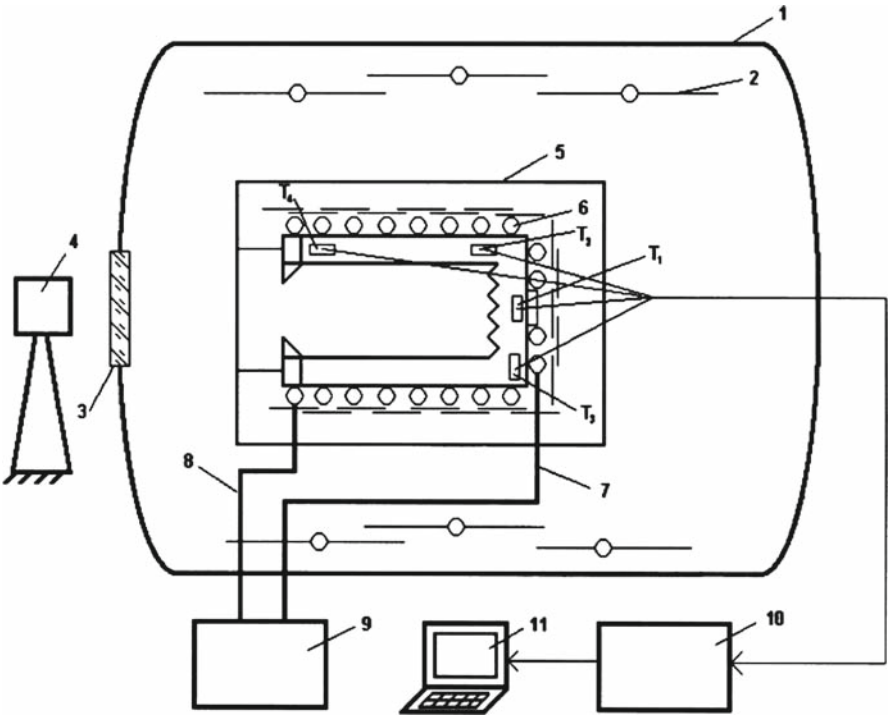

Fig. 5 Schematic of location of BB100-V1 with its PRT sensors in FTVT vacuum chamber: (1) FTVT chamber wall; (2) LN_2 screens; (3) IR window of FTVT chamber (material of window—KRS); (4) Thermoimager AGA-780; (5) BB100-V1 housing; (6) Tubing for KRYO-51 liquid; (7) Input of heat-transfer liquid; (8) Output of heat-transfer liquid; (9) LAUDA RP1845 thermostat; (10) Multimeter HP-34970A with scanner card "HP 34901A"; and (11) Monitoring PC (notebook) with RS232 port

BB-80/350 represents a plane radiation source with a black-painted radiating surface. This paint features an emissivity of a known high enough value. In operation, the thermal radiation source is placed inside a chamber filled with dry nitrogen, or into a vacuum chamber. BB-80/350 consists of a heated radiation surface and a heat exchanger linked to the radiation surface with supports serving as thermal resistors. Feedback sensors (PRT-100 resistors) of the thermal control system and temperature monitoring system sensor are located on the BB-80/350 radiating surface.

The BB-80/350 radiating surface is heated with heating coils aligned with the thermal resistance supports. The BB-80/350 radiating surface is cooled by passing liquid nitrogen vapor through the heat exchanger. When operated at high temperature ($>300\,K$), the nitrogen vapor delivery to the heat exchanger may be stopped.

The nonoperating side of the BB-80/350 radiation surface and heat exchanger are covered with thermal insulation designed for instrument operation at atmospheric pressure (in dry air or nitrogen atmosphere). To provide for BB-80/350 operation in a vacuum chamber, the thermal insulation is replaced with multilayer screen-vacuum insulation.

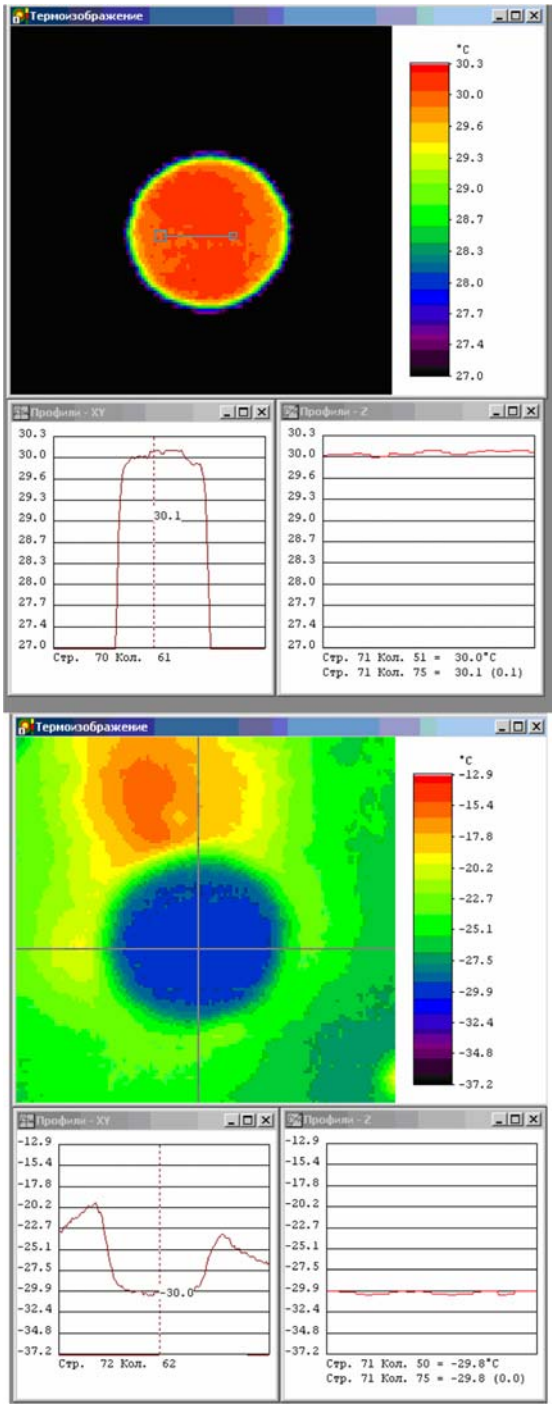

Fig. 6 BB100-V1 aperture scan at $T = +30\,^{\circ}\mathrm{C}$ (*left*) and $-30\,^{\circ}\mathrm{C}$ (*right*). Determination of the spatial distribution of radiation temperature across the aperture of the BB100-V1 was performed by means of a thermal imager, AGA-780, placed in the vicinity of the IR-window outside the cryo-vacuum chamber

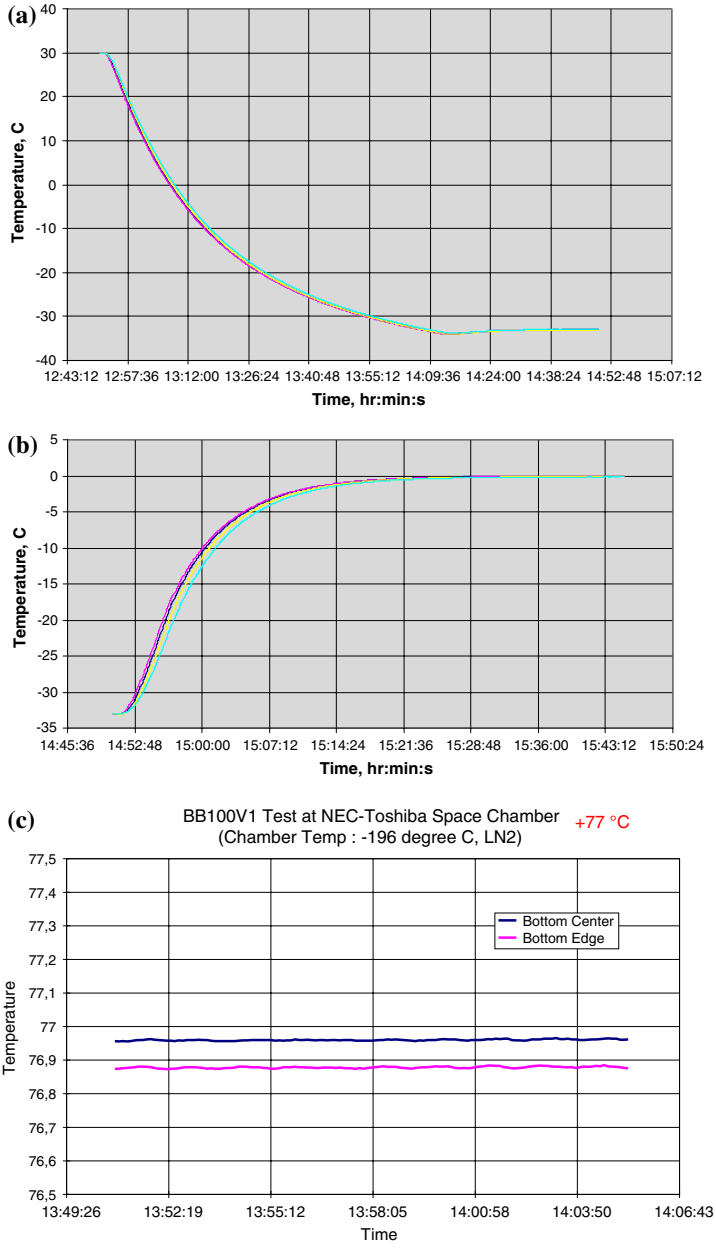

Fig. 7 Operation of temperature-monitoring system of BB100-V1 at the set-point temperatures −33 °C (240 K), 0 °C, +30 °C, and +77 °C (350 K). Results of temperature measurements from PRT-100 sensors calibrated by MINCO (USA): (bf a) transition from $T = +30$ °C to 33 °C, and stabilization at the set point of −33 °C (240 K). KELDYSH Center. Environment: vacuum Keldysh Space chamber, cooled with LN_2, (**b**) transition from $T = -33$ °C to 0 °C, and stabilization at the set point of 0 °C. Keldysh Center, and (**c**) thermostabilization at 77 °C in NEC-Toshiba chamber cooled with LN_2. Discrepancy between center and edge of cavity bottom is <0.04 K

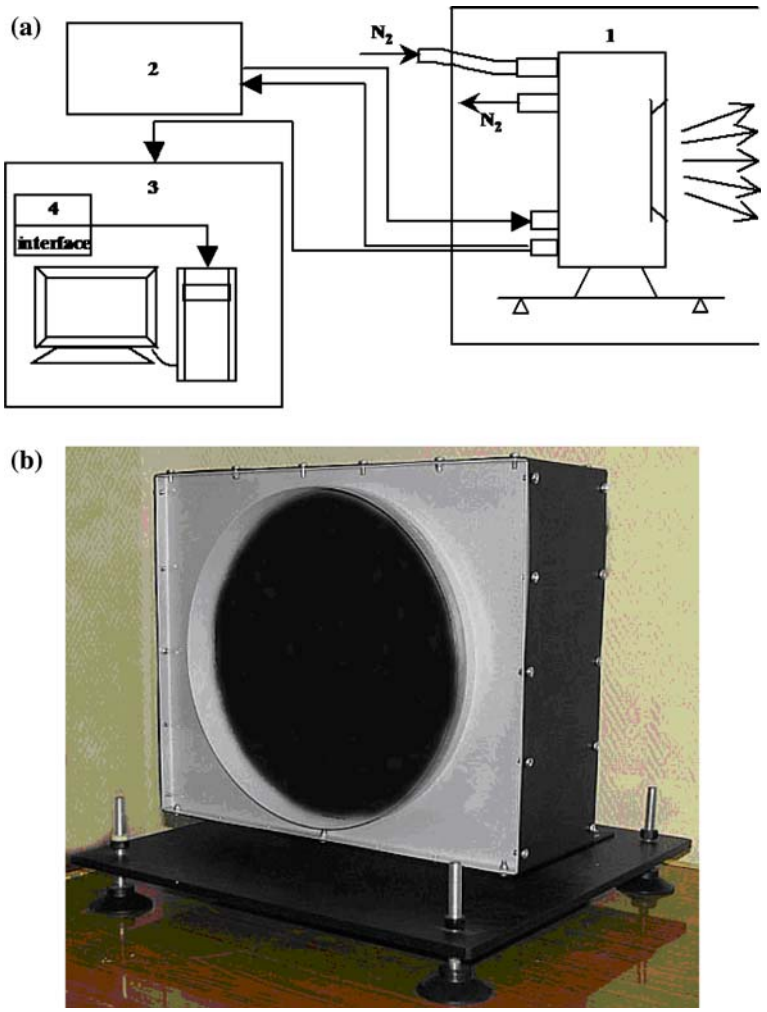

Fig. 8 (**a**) BB-80/350 diagram: (1) BB-80/350; (2) thermostabilization system; (3) temperature monitoring system; (4) voltmeter and (**b**) BB-80/350 layout

The thermal controlling system and parameter monitoring system of the heat radiation source are located outside the chamber. The thermal conditioning system of the radiation source is designed for setting and maintaining the required BB-80/350 temperature and consists of the sensor located on the radiation surface and the control unit containing the microprocessor-based temperature regulator and power supply unit providing the heaters' power supply. The thermal conditioning system also includes the device that supplies nitrogen vapor to the BB-80/350 heat exchanger, its power supply unit, and the nitrogen vapor piping. The device is an evaporator placed into a vessel containing liquid nitrogen. The temperature control unit consists of a microprocessor-based temperature regulator and solid-state relay and power supply.

Table 4 Basic BB-80/350 features

Parameter	Value
Operating temperature range	(220 to 350) K
Working aperture	350 mm
Spectral range	(2.5–15) μm
Emissivity	0.96 ± 0.02
Maximum temperature instability under thermostabilization	0.1 K
Temperature nonuniformity across opening (at 280. . .300 K)	±0.1 K
Time period of temperature change on 5 K	<10 min
Continuous operation time	8 h
Input voltage	220 V AC
Frequency	50 Hz
Working conditions:	
(1) In housing	Dry Argon gas atmosphere, normalized pressure; environment temperature range 0…30 °C ;
(2) In vacuum chamber	$P = 10^{-5} \ldots 10^{-6}$ Torr; Temperature of chamber walls 77 K
Consumed power:	
(1) With thermostabilization system:	<500 W
(2) With evaporator	<800 W
Weight	29 kg (57 kg with adjustment support)
Dimensions	200 mm × 400 mm × 460 mm (500 mm × 600 mm × 460 mm with adjustment support)

The microprocessor-based temperature regulator Dicon 500 703570/082-111-223355-23-54/00,61 made by JUMO Mess- und Regeltechnik, Germany is used to set the radiation source temperature, to indicate the current temperature value, and to maintain the assigned temperature with the required accuracy. The control signal from the microprocessor temperature regulator is connected to a solid-state relay, which controls the radiation source heating current. The solid-state relay provides PID control of the heater power.

The parameter monitoring system is designed for online temperature monitoring of the radiation source and consists of the sensor located on the BB-80/350 radiation surface, a digital voltmeter, the interface unit, and a computer for visualization, storage, and data processing.

A visual representation of sample scans across the BB-80/350 aperture obtained by means of a thermal imager (ThermoPro-TP8 by Wuhan Guide Infrared Technology Co., Ltd, China) under ambient air conditions is shown in Fig. 9. The BB-80/350 emissivity estimated by means of STEEP3 software on the basis of the known emissivity of Nextel Velvet 821-11 black paint cover is 0.96 ± 0.02.

Results of BB-80/350 stabilization tests at ≈29 °C and 73 °C temperature set-point values in air environmental conditions are as follows:

Maximum temperature instability under thermostabilization	0.1 K
Temperature nonuniformity across opening (at 280 K to 300 K)	±0.1 K
Time required to change temperature by 5 K	<10 min.

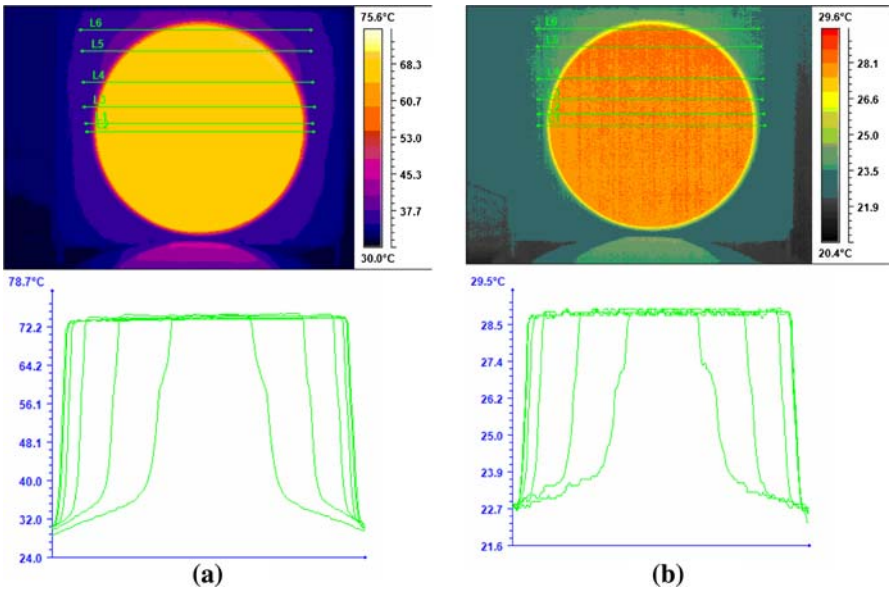

Fig. 9 Spatial distribution of radiation temperature across the aperture of BB-80/350 by means of thermal imager ThermoPro-TP8 (by Wuhan Guide Infrared Technology Co., Ltd, China) placed a distance of 3 m from the blackbody radiating surface; ambient air environment temperature was 31 °C: (**a**) BB-80/350 aperture scan at $T = 72.2$ °C and (**b**) aperture scan at $T = 28.8$ °C

2.4 Low-Temperature Fixed Points on the Basis of Phase Transitions of Pure Metals and Metal–Metal Eutectics

To meet the requirements for reproducibility and admissible uncertainty of measurements for the reference radiometric equipment used for the calibration of space-born radiometric instruments, it became necessary to develop low-temperature fixed points in the temperature range from 10.5 °C to 30 °C based on the phase transition of single-component substances, e.g., Ga, and inter-metallic eutectic alloys such as GaInSn, GaIn, GaSn, GaZn, and GaAl [1,2]. Fixed points are widely studied and used for ground-based thermometry and radiometry, and they possess potentially unique reproducibility of radiometric characteristics ensuing from the repeatability of the phase-transition temperature in itself. The influence of external forces from bringing the spaceship onto orbit as well as from the factors of space flight make it necessary to ensure the constancy of the characteristics of the equipment; the use of phase transitions of single-component substances and eutectic alloys has been investigated for this purpose.

Within the temperature range from 300 K to 450 K, reference temperatures can be provided by the single-component metals Ga and In and various eutectic alloys based on these metals [1,2], e.g., GaInSn (melting temperature about 10.8 °C), GaIn (about 15.7 °C), GaSn (about 20.5 °C), GaZn (about 25.3 °C), GaAl (about 27 °C), GaCd (about 29.4 °C), and, possibly, InBi (about 72.7 °C).

The widening of the temperature interval between fixed points increases the accuracy of calibrations. That's why it is advisable to select one fixed point out of the eutectics GaCd, GaAl, GaZn (or pure Ga); the other from GaIn, GaSn, or GaInSn with a lower melting temperature. Another variant is possible as well: one point using gallium or eutectics based on gallium, and another one based on indium or InBi. In doing so, at the stage of the laboratory (ground-based) experiments for research and selection of expected fixed points, it is sufficient to use regular methods for the Ga melting fixed-point realization.

VNIIOFI has gained experience in prelaunch testing of the metrological characteristics of low-temperature fixed-point alloys based on Ga [1,2]. Five promising low-temperature fixed points for application in IR preflight calibrations - Ga (302.9146 K), and the eutectics GaIn (288.806 K), GaSn (293.662 K), GaZn (298.42 K), and GaAl (300.08 K) have been investigated. The detailed description of our experiments with such fixed points was presented at TEMPMEKO 2007 [24].

Some brief results are as follows: it was discovered that deep supercooling (during solidification of Ga placed in a small Teflon cell containing about 120 g of metal) is absent. The reproducibility of melting plateaux of gallium in small crucibles is about 0.5 mK. This made it possible to utilize the melting fixed point of Ga realized in a small cell for in-flight calibrations. As the second reference point for carrying out radiometric calibrations during space flight, it is expedient to use the fixed point of the GaIn eutectic alloy featuring a reproducibility of about 1 mK.

3 Results

For the last 30 years, VNIIOFI has developed a wide range of precision low-temperature BB radiation sources covering the wavelength range from 0.2 µm to 15 µm.

The new family of research-grade low-temperature BBs (240 K to 350 K) was developed for high-accuracy IR preflight calibration of space-borne instruments featuring apertures from 100 mm to 350 mm. The temperature nonuniformity and long-term stability of variable-temperature (240 to 350) K BB100-V1 at 100 mm aperture are <0.1 K and 0.1 % (from 1.5 µm to 15 µm) under the cryo-vacuum conditions of a medium-background environment.

Application of new BBs based on low-temperature binary eutectic alloys enables the solution of numerous topical problems of space and astrophysical investigations (including solar constant monitoring with a measurement uncertainty of <0.1 % per decade), as well as ecology, climatology, unique measurements within the framework of GEOSS, and improvement of calibration accuracy of space-borne radiometric instruments. An anticipated accuracy improvement of 1.5 to 2 times is anticipated compared to the currently attained level.

References

1. V.N. Krutikov, V.I. Sapritsky, B.B. Khlevnoy, B.E. Lisiansky, S.P. Morozova, S.A. Ogarev, A.S. Panfilov, M.K. Sakharov, M.L. Samoylov, G. Bingham, T. Humphreys, A. Thurgood, V.E. Privalsky, Metrologia **43**, 2 (2006)

2. V. Sapritsky, B. Khlevnoy, S. Ogarev, V. Privalsky, M. Samoylov, M. Sakharov, A. Bourdakin, A. Panfilov, in *SPIE "InfraRed Spaceborne Remote Sensing XIV" Conference*, San Diego, 2006, Paper No. 6297–34
3. V.I. Sapritsky, Metrologia **32**, 411 (1995/1996)
4. H.W. Yoon, C.E. Gibson, J.L. Gardner, in *Temperature, Its Measurement and Control in Science and Industry*, vol. 7, ed. by D.C. Ripple (AIP, Melville, NY, 2003), pp. 601–606
5. V.I. Sapritsky, S.A. Ogarev, B.B. Khlevnoy, M.L. Samoylov, V.B. Khromchenko, in *Temperature, Its Measurement and Control in Science and Industry*, vol. 7, ed. by D.C. Ripple (AIP, Melville, NY, 2003), pp. 273–277
6. V.I. Sapritsky, S.A. Ogarev, B.B. Khlevnoy, M.L. Samoylov, V.B. Khromchenko, S.P. Morozova, in *Proceedings of SPIE IR Spaceborne Remote Sensing X Conference*, vol. 4818, Seattle, Washington, 2002, pp. 127–136
7. V.I. Sapritsky, M.K. Sakharov, S.P. Morozova, B.E. Lisiansky, S.A. Ogarev, B.B. Khlevnoy, A.S. Panfilov, in *Conference CD of CALCON'2004 (Conference on Characterization and Radiometric Calibration for Remote Sensing)* (Utah State University, Logan, UT, 2004)
8. V.I. Sapritsky, V.B. Khromchenko, S.N. Mekhontsev, M.L. Samoilov, A.V. Prokhorov, S.A. Ogarev, A. Shumway, in *Conference CD of CALCON'2000* (Utah State University, Logan, UT, 2000)
9. V.I. Sapritsky, A.V. Prokhorov, Metrologia **29**, 9 (1992)
10. STEEP3, Version 1.3. *User's Guide* (Virial, Inc., NY, 2000)
11. S. Moaveni, *Finite Element Analysis: Theory and Applications with ANSYS*, 2nd edn. (Prentice Hall, Upper Saddle River, NJ, 2003)
12. V.I. Sapritsky, A.V. Prokhorov, Appl. Optics **34**, 5645 (1995)
13. A.V. Murthy, A.V. Prokhorov, D.P. DeWitt, J. Thermophys. Heat Trans. **18**, 333 (2004)
14. R.D. Siegel, J.R. Howell, *Thermal Radiation Heat Transfer*, 3rd edn. (Hemisphere, Washington, DC, 1992)
15. S.M. Pompea, R.P. Breault, in *Handbook of Optics*, vol. 2 (McGraw-Hill, New York, 1995), pp. 37.1–37.63
16. D.B. Betts, F.J.J. Clarke, L.J. Cox, J.A. Larkin, J. Phys. E: Sci. Instrum. **18**, 689 (1985)
17. A.A. De Silva, B.W. Jones, Sol. Energ. Mater. **15**, 391 (1987)
18. J. Envall, P. Kärhä, E. Ikonen, Metrologia **41**, 353 (2004)
19. B.E. Wood, J.G. Pipes, A.M. Smith, J.A. Roux, Appl. Optics **15**, 940 (1976)
20. M. Batuello, S. Clausen, J. Hameury, P. Bloembergen, in *Proceedings of TEMPMEKO '99, 7th International Symposium on Temperature and Thermal Measurements in Industry and Science*, ed. by J. F. Dubbeldam, M.J. de Groot (Edauw Johannissen bv, Delft, 1999), pp. 601–606
21. J. Lohrengel, R. Todtenhaupt, PTB-Mitteilungen (RAL 900 15 tiefschwarz matt) **106**, 259 (1996)
22. Mankiewicz Gebr. & Co., Georg-Wilhelm-Straße 189, 21107 Hamburg, Germany. E-mail: info@mankiewicz.de
23. S. Ogarev, M. Samoylov, V. Sapritsky, A. Panfilov, S. Koichi, T. Kawashima, in *Proceedings of NEWRAD'2005*, Davos, Switzerland, 2005, Paper 083
24. A. Burdakin, B. Khlevnoy, M. Samoylov, V. Sapritsky, S. Ogarev, A. Panfilov, S. Prokhorenko, in *Proceedings of TEMPMEKO 2007*, Int. J. Thermophys., doi: 10.1007/s10765-008-0441-x